

# Entanglement dynamics for Unruh-DeWitt detectors interacting with massive scalar fields: The Unruh and anti-Unruh effects

Yuebing Zhou<sup>1,2</sup>, Jiawei Hu<sup>1\*</sup> and Hongwei Yu<sup>1†</sup>

<sup>1</sup>*Department of Physics and Synergetic Innovation*

*Center for Quantum Effects and Applications,*

*Hunan Normal University, Changsha, Hunan 410081, China*

<sup>2</sup>*Department of Physics, Huaihua University, Huaihua, Hunan 418008, China*

## Abstract

We study, in the framework of open quantum systems, the entanglement dynamics for a quantum system composed of two uniformly accelerated Unruh-Dewitt detectors interacting with a bath of massive scalar fields in the Minkowski vacuum. We find that the entanglement evolution for the quantum system coupled with massive fields is always slower compared with that of the one coupled with massless fields, and this time-delay effect brought by the field being massive can however be counteracted by a large enough acceleration, in contrast to the case of a static quantum system in a thermal bath, where this time delay is not affected by the temperature. Remarkably, the maximal concurrence of the quantum system generated during evolution may increase with acceleration for any inter-detector separation while that for static ones in a thermal bath decreases monotonically with temperature, and this can be considered as an anti-Unruh effect in terms of the entanglement generated.

---

\* Corresponding author: jwhu@hunnu.edu.cn

† Corresponding author: hwyu@hunnu.edu.cn

## I. INTRODUCTION

Quantum field theory predicts that a uniformly accelerated observer perceives the vacuum of an inertial observer as a thermal bath at a temperature proportional to its proper acceleration, which is known as the Unruh effect [1–4]. A widely used model of uniformly accelerated observers is the Unruh-DeWitt detector, which is typically modeled as a point-like two-level quantum system coupled with fluctuating vacuum quantum fields [3, 5]. In fact, the thermal bath perceived by the uniformly accelerated observer can be considered as the Rindler thermal bath, which may not necessarily be same as the Minkowski thermal bath seen by an inertial observer. Many studies have been committed to comparing the different behaviors between quantum systems immersed in the two kinds of thermal baths from different physical aspects, e.g. the spontaneous emission rates [6–9], the Lamb shifts [10, 11], the resonance interactions [12, 13] and the Casimir-Polder interactions [14–16]. It has been shown that, only in some special situations, the behaviors of a single Unruh-DeWitt detector in the two kinds of thermal baths are equivalent, such as in the case of massless scalar fields in a free spacetime [7, 10].

Recently, the influences of environment on the entanglement dynamics of an open quantum system have been extensively studied, such as those leading to the environment-induced entanglement sudden death [17, 18], entanglement revival [19] and entanglement creation [20–32]. Therefore, a question naturally arises as to how the entanglement dynamics of a quantum system composed of two Unruh-DeWitt detectors will be affected by acceleration, and how will it be different from that of a static one in a thermal bath in the Minkowski spacetime at the Unruh temperature related to acceleration. In Ref. [33], the entanglement generation of two uniformly accelerated Unruh-DeWitt detectors coupled with fluctuating massless scalar fields in the Minkowski vacuum with a vanishing separation has been studied, and it has been shown that the asymptotic entanglement is exactly the same as that immersed in a thermal bath at the Unruh temperature. However, in more general cases, e.g. when the separation between the detectors is nonzero [34–36], in the presence of a boundary [36, 37], and for the quantum systems coupled with different kinds of quantum fields, such as electromagnetic fields [35, 36], the differences between the entanglement dynamics of an accelerated quantum system and that of a static one in a thermal bath show up.

When an Unruh-DeWitt detector is coupled with massive scalar fields, transitions among

different eigenstates for an accelerated detector can still occur even when the mass of the field is greater than the energy level spacing of the detector [4, 6, 8], which is impossible for a static one in a thermal bath. Furthermore, it has been shown in Ref. [38] that the mass of the field will bring a gray factor related to acceleration to the transition rate of an Unruh-DeWitt detector, which results in the fact that the transition rate may decrease with acceleration. Later, this phenomenon is named as the anti-Unruh effect [39, 40]. Recently, the entanglement dynamics of two static detectors coupled with massive scalar fields has been studied in Ref. [41]. It has been found that, compared with the massless field case, the evolution of entanglement is slower and the region of spatial separation between the detectors within which entanglement can be generated is significantly enlarged. This means that it is possible to achieve long-distance entanglement generation and long-lived entanglement. Now, a natural question is, will there be essential differences between the behaviors of two uniformly accelerated Unruh-DeWitt detectors coupled with massive fields in the Minkowski vacuum and that of a static one in a thermal bath in terms of entanglement dynamics? In particular, will there be anti-Unruh phenomena, e.g. the entanglement generated for accelerated detectors increases with acceleration, while that for static ones in a thermal bath decreases with temperature? In the present paper, we study, in the framework of open quantum systems, the entanglement dynamics for a uniformly accelerated quantum system composed of two Unruh-DeWitt detectors interacting with a bath of fluctuating massive scalar fields in the Minkowski vacuum. Hereafter natural units with  $\hbar = c = k_B = 1$  are used unless specified, where  $c$  is the speed of light,  $\hbar$  the reduced Planck constant, and  $k_B$  the Boltzmann constant.

## II. THE BASIC FORMALISM

We consider a quantum system composed of a pair of Unruh-DeWitt detectors in interaction with a bath of fluctuating massive scalar fields in the Minkowski vacuum. The Hamiltonian of the total system takes the form

$$H = H_S + H_F + H_I. \quad (1)$$

Here  $H_S$  denotes the Hamiltonian of the quantum system, which can be written as

$$H_S = \frac{\omega}{2}\sigma_3^{(1)} + \frac{\omega}{2}\sigma_3^{(2)}, \quad (2)$$

where  $\omega$  is the energy level spacing,  $\sigma_i^{(1)} = \sigma_i \otimes \sigma_0$ ,  $\sigma_i^{(2)} = \sigma_0 \otimes \sigma_i$ , with  $\sigma_i$  ( $i = 1, 2, 3$ ) being the Pauli matrices, and  $\sigma_0$  the  $2 \times 2$  unit matrix.  $H_F$  is the Hamiltonian of the massive scalar fields. The interaction Hamiltonian  $H_I$  can be written in analogy to the electric dipole interaction as [7]

$$H_I = \mu[\sigma_2^{(1)}\phi(t_1, \mathbf{x}_1) + \sigma_2^{(2)}\phi(t_2, \mathbf{x}_2)], \quad (3)$$

where  $\mu$  is the coupling constant which is assumed to be small, and  $\phi(t, \mathbf{x})$  is the field operator.

We assume that initially the quantum system is uncorrelated with the environment, i.e., the initial state of the total system can be written as  $\rho_{\text{tot}}(0) = \rho(0) \otimes |0\rangle\langle 0|$ , where  $|0\rangle$  is the vacuum state of the massive scalar fields, and  $\rho(0)$  denotes the initial state of the quantum system. The density matrix of the total system satisfies the Liouville equation

$$\frac{\partial \rho_{\text{tot}}(\tau)}{\partial \tau} = -i[H, \rho_{\text{tot}}(\tau)]. \quad (4)$$

Under the Born-Markov approximation, the reduced density matrix of the quantum system  $\rho(\tau) = \text{Tr}_F[\rho_{\text{tot}}(\tau)]$  can be described by the Gorini-Kossakowski-Lindblad-Sudarshan (GKLS) master equation [42, 43],

$$\frac{\partial \rho(\tau)}{\partial \tau} = -i[H_{\text{eff}}, \rho(\tau)] + \mathcal{D}[\rho(\tau)]. \quad (5)$$

$H_{\text{eff}}$  and  $\mathcal{D}[\rho(\tau)]$  in the equation above are the effective Hamiltonian and the dissipative term respectively, whose explicit form can be written as

$$H_{\text{eff}} = H_S - \frac{i}{2} \sum_{\alpha, \varrho=1}^2 \left[ H_+^{(\alpha\varrho)} \sigma_+^{(\alpha)} \sigma_-^{(\varrho)} + H_-^{(\alpha\varrho)} \sigma_-^{(\alpha)} \sigma_+^{(\varrho)} \right],$$

and

$$\begin{aligned} \mathcal{D}[\rho(\tau)] = & \frac{1}{2} \sum_{\alpha, \varrho=1}^2 \left[ D_+^{(\alpha\varrho)} \left( 2\sigma_-^{(\varrho)} \rho \sigma_+^{(\alpha)} - \{\sigma_+^{(\alpha)} \sigma_-^{(\varrho)}, \rho\} \right) \right. \\ & \left. + D_-^{(\alpha\varrho)} \left( 2\sigma_+^{(\varrho)} \rho \sigma_-^{(\alpha)} - \{\sigma_-^{(\alpha)} \sigma_+^{(\varrho)}, \rho\} \right) \right], \end{aligned} \quad (6)$$

where  $\sigma_{\pm}^{(1)} = \sigma_{\pm} \otimes \sigma_0$  and  $\sigma_{\pm}^{(2)} = \sigma_0 \otimes \sigma_{\pm}$  with  $\sigma_- = |0\rangle\langle 1|$ ,  $\sigma_+ = |1\rangle\langle 0|$ . Here,  $D_{\pm}^{(\alpha\varrho)}$  and  $H_{\pm}^{(\alpha\varrho)}$  are determined by  $C^{(\alpha\varrho)}(\tau - \tau')$  and  $\chi^{(\alpha\varrho)}(\tau - \tau')$ , which are the symmetric and antisymmetric correlation functions of the fields

$$\begin{aligned} C^{(\alpha\varrho)}(\Delta\tau) &= \frac{1}{2} \langle \{\phi(t_{\alpha}(\tau), \mathbf{x}_{\alpha}(\tau)), \phi(t_{\varrho}(\tau'), \mathbf{x}_{\varrho}(\tau'))\} \rangle, \\ \chi^{(\alpha\varrho)}(\Delta\tau) &= \frac{1}{2} \langle [\phi(t_{\alpha}(\tau), \mathbf{x}_{\alpha}(\tau)), \phi(t_{\varrho}(\tau'), \mathbf{x}_{\varrho}(\tau'))] \rangle. \end{aligned} \quad (7)$$

Note here that,  $\langle \cdot \cdot \cdot \rangle$  denotes the expectation value with respect to a certain state of the quantum field, and  $\{\cdot, \cdot\}$ ,  $[\cdot, \cdot]$  are the anti-commutator and commutator of two operators respectively. Moreover, since the environment perceived by the quantum system is stationary, the correlation functions of the fields are functions of  $\Delta\tau = \tau - \tau'$ , see Eq. (7). Then, the emission coefficient  $D_+^{(\alpha\varrho)}$  and absorption coefficient  $D_-^{(\alpha\varrho)}$  can be written as

$$D_{\pm}^{(\alpha\varrho)} = \frac{1}{2} [\mathcal{F}_C^{(\alpha\varrho)}(\omega) \pm \mathcal{F}_{\chi}^{(\alpha\varrho)}(\omega)], \quad (8)$$

where  $\mathcal{F}_C^{(\alpha\varrho)}(\omega)$  and  $\mathcal{F}_{\chi}^{(\alpha\varrho)}(\omega)$ , which are respectively related to the Fourier transforms of the symmetric and antisymmetric correlation functions, can be expressed as

$$\mathcal{F}_C^{(\alpha\varrho)}(\omega) = 2\mu^2 \int_{-\infty}^{\infty} C^{(\alpha\varrho)}(\Delta\tau) e^{i\omega\Delta\tau} d\Delta\tau, \quad (9)$$

$$\mathcal{F}_{\chi}^{(\alpha\varrho)}(\omega) = 2\mu^2 \int_{-\infty}^{\infty} \chi^{(\alpha\varrho)}(\Delta\tau) e^{i\omega\Delta\tau} d\Delta\tau. \quad (10)$$

Similarly,  $H_{\pm}^{(\alpha\varrho)}$  can be obtained by replacing  $C^{(\alpha\varrho)}(\Delta\tau)$  with  $\chi^{(\alpha\varrho)}(\Delta\tau) \text{sign}(\Delta\tau)$  and  $\chi^{(\alpha\varrho)}(\Delta\tau)$  with  $C^{(\alpha\varrho)}(\Delta\tau) \text{sign}(\Delta\tau)$  respectively, where  $\text{sign}(\Delta\tau)$  is the sign function which equals to  $-1, 0, 1$  when  $\Delta\tau <, =, > 0$  respectively.

In the following, we define three dimensionless physical parameters using  $\mathcal{F}_{C(\chi)}^{(\alpha\varrho)}(\omega)$  to describe the entanglement dynamics of the quantum system.

1.  $\Omega$ . The factor  $\Omega$  is defined as

$$\Omega = \frac{\mathcal{F}_{\chi}^{(\alpha\alpha)}(\omega)}{\mathcal{F}_{\chi}^{(\alpha\alpha)}(\omega)|_{m=0}}, \quad (11)$$

which represents the ratio of the spontaneous emission rate of an Unruh-DeWitt detector coupled with massive scalar fields to that of the one coupled with massless scalar fields. Here, the spontaneous emission rate of the Unruh-DeWitt detector coupled to massless scalar fields in the Minkowski vacuum is  $\Gamma_0 \equiv \mathcal{F}_{\chi}^{(11)}(\omega)|_{m=0} = \mathcal{F}_{\chi}^{(22)}(\omega)|_{m=0} = \mu^2\omega/2\pi$ .

In the acceleration case, we can obtain

$$\Omega_a = \frac{\sinh(\pi\omega/a)}{\pi\omega/a} \frac{m^2}{a^2} [K_{1+i\omega/a}(m/a) K_{-1+i\omega/a}(m/a) - K_{i\omega/a}^2(m/a)], \quad (12)$$

where  $K_{\nu}(x)$  is the second type of modified Bessel function (refer to Appendix A for details). For the convenience of later discussions,  $\Omega_a$  is written as a function of dimensionless variables as  $\Omega_a(m/\omega, a/\omega)$ . For comparison, in the thermal bath case,  $\Omega_{\beta}$  can be obtained as

$$\Omega_{\beta} = \begin{cases} \sqrt{1 - \frac{m^2}{\omega^2}}, & \omega > m, \\ 0, & \omega \leq m. \end{cases} \quad (13)$$

In both the two cases, one can prove that  $\Omega \in [0, 1]$ , with  $\Omega = 1$  corresponding to the massless case. One can refer to Appendix A for the derivations of Eqs. (12) and (13).

2.  $\eta$ . If the environment is in an equilibrium state which satisfies the Kubo-Martin-Schwinger (KMS) condition [44–46] (which is true for the models considered in the present paper), the Wightman function satisfies the following property

$$G^+(\Delta\tau - i\beta_K) = G^+(-\Delta\tau), \quad (14)$$

where  $\beta_K = 1/T_K$  is a positive parameter called the inverse KMS temperature. Then, we can obtain that  $\mathcal{G}^+(-\omega) = e^{-\beta_K\omega}\mathcal{G}^+(\omega)$ , where  $\mathcal{G}^+(\omega) = \int_{-\infty}^{\infty} G^+(\Delta\tau) e^{i\omega\Delta\tau} d\Delta\tau$ , and define a dimensionless factor  $\eta$  as

$$\eta = \frac{\mathcal{F}_C^{(\alpha\varrho)}(\omega)}{\mathcal{F}_\chi^{(\alpha\varrho)}(\omega)} = \frac{e^{\omega\beta_K} + 1}{e^{\omega\beta_K} - 1} = \coth \frac{\omega\beta_K}{2}. \quad (15)$$

The factor  $\eta$  can be re-expressed with the downward and upward transition rates  $\mathcal{R}^\downarrow = \mathcal{R}_{|k\rangle \rightarrow |l\rangle}$ ,  $\mathcal{R}^\uparrow = \mathcal{R}_{|l\rangle \rightarrow |k\rangle}$  between any two energy eigenstate  $|k\rangle$  (high), and  $|l\rangle$  (low) as

$$\eta = \frac{\mathcal{R}^\downarrow + \mathcal{R}^\uparrow}{\mathcal{R}^\downarrow - \mathcal{R}^\uparrow} = 2N_K + 1 = \coth \frac{\omega}{2T_K}, \quad (16)$$

where  $N_K$  is the effective particle number, and the KMS temperature  $T_K = 1/\beta_K = \omega [\ln(1 + 1/N_K)]^{-1}$ . For the acceleration case,  $\eta_a = \coth \frac{\pi\omega}{a} = \coth \frac{\omega}{2T_U}$ , where  $T_U = \frac{a}{2\pi}$  is the Unruh temperature, and for the thermal bath case  $\eta_\beta = \coth \frac{\beta\omega}{2} = \coth \frac{\omega}{2T}$  (see Appendix A for details). Moreover, it is obvious that  $\eta \in [1, +\infty]$ , with  $\eta = 1$  corresponding to the case when the (Unruh) temperature is zero.

3.  $\lambda$ . In our model,  $\mathcal{F}_\chi^{(11)}(\omega) = \mathcal{F}_\chi^{(22)}(\omega)$  and  $\mathcal{F}_\chi^{(12)}(\omega) = \mathcal{F}_\chi^{(21)}(\omega)$ . Then we can define a factor  $\lambda$  as

$$\lambda = \frac{\mathcal{F}_\chi^{(\alpha\varrho)}(\omega)|_{\alpha \neq \varrho}}{\mathcal{F}_\chi^{(\alpha\varrho)}(\omega)|_{\alpha = \varrho}}, \quad (17)$$

Similarly, the factor  $\lambda$  can be re-expressed with the upward and downward collective transition rates related to the symmetric state  $|S\rangle = \frac{1}{\sqrt{2}}(|10\rangle + |01\rangle)$  and anti-symmetric state  $|A\rangle = \frac{1}{\sqrt{2}}(|10\rangle - |01\rangle)$  as

$$\lambda = \frac{\mathcal{R}_S^\downarrow - \mathcal{R}_A^\downarrow}{\mathcal{R}_S^\downarrow + \mathcal{R}_A^\downarrow} = \frac{\mathcal{R}_S^\uparrow - \mathcal{R}_A^\uparrow}{\mathcal{R}_S^\uparrow + \mathcal{R}_A^\uparrow}. \quad (18)$$

Here, these collective rates are respectively  $\mathcal{R}_S^\downarrow = \mathcal{R}_{|E\rangle \rightarrow |S\rangle} = \mathcal{R}_{|S\rangle \rightarrow |G\rangle}$ ,  $\mathcal{R}_A^\downarrow = \mathcal{R}_{|E\rangle \rightarrow |A\rangle} = \mathcal{R}_{|A\rangle \rightarrow |G\rangle}$ ,  $\mathcal{R}_S^\uparrow = \mathcal{R}_{|G\rangle \rightarrow |S\rangle} = \mathcal{R}_{|S\rangle \rightarrow |E\rangle}$  and  $\mathcal{R}_A^\uparrow = \mathcal{R}_{|G\rangle \rightarrow |A\rangle} = \mathcal{R}_{|A\rangle \rightarrow |E\rangle}$ , with  $|E\rangle = |11\rangle$  and  $|G\rangle = |00\rangle$ . From Eq. (18), it is straightforward to show that  $|\lambda| \leq 1$ . For the acceleration case,  $\lambda_a$  can be obtained as

$$\lambda_a = \frac{4a^2}{m^2} \frac{\int_{\frac{m}{a}}^{\infty} \frac{1}{aL} \sin(aL\sqrt{x^2 - m^2/a^2}) K_{i2\omega/a}(2x) dx}{K_{1+i\omega/a}(m/a) K_{-1+i\omega/a}(m/a) - K_{i\omega/a}^2(m/a)}, \quad (19)$$

which can be written as a function of dimensionless variables as  $\lambda_a(m/\omega, a/\omega, \omega L)$ . For the thermal bath case,

$$\lambda_\beta = \frac{\sin(\omega L \Omega_\beta)}{\omega L \Omega_\beta}. \quad (20)$$

Recall that  $\Omega_\beta$  has been given in Eq. (13). The derivations of Eqs. (19) and (20) are given in Appendix A.

With the parameters defined above,  $D_\pm^{(\alpha\varrho)}$  in Eq. (8) can be re-expressed as

$$\begin{aligned} D_\pm^{(11)} &= D_\pm^{(22)} = \frac{1}{2}(\eta \pm 1) \Omega \Gamma_0, \\ D_\pm^{(12)} &= D_\pm^{(21)} = \frac{1}{2}(\eta \pm 1) \lambda \Omega \Gamma_0. \end{aligned} \quad (21)$$

Now, we choose to work in the coupled basis  $\{|E\rangle, |S\rangle, |A\rangle, |G\rangle\}$ , where  $|E\rangle = |11\rangle$ ,  $|S\rangle = \frac{1}{\sqrt{2}}(|10\rangle + |01\rangle)$ ,  $|A\rangle = \frac{1}{\sqrt{2}}(|10\rangle - |01\rangle)$  and  $|G\rangle = |00\rangle$ . For simplicity, we assume that the initial density matrix is in the X form, i.e. the only nonzero elements are those along the diagonal and anti-diagonal of the density matrix in the coupled basis  $\{|E\rangle, |S\rangle, |A\rangle, |G\rangle\}$ , then the X form will be maintained during evolution [47]. Now, a set of equations which describe the time evolution of the density matrix elements can be expressed as

$$\dot{\mathbf{X}}(\tau) = -\mathbf{U}(\eta, \lambda) \mathbf{X}(\tau); \quad \dot{\rho}_{IJ}(\tau) = -\rho_{IJ}(\tau), \quad (22)$$

where  $\rho_{IJ}(\tau) = \langle I | \rho(\tau) | J \rangle$ ,  $I, J \in \{G, E, A, S\}$ , and  $\dot{\rho}_{IJ}(\tau) = d\rho_{IJ}(\tau)/d\zeta$  is the derivative with respect to the dimensionless time  $\zeta = \eta \Omega \Gamma_0 \tau$ . The column vector  $\mathbf{X}(\tau)$  is defined as  $\mathbf{X}(\tau) = (\rho_E(\tau) \ \rho_S(\tau) \ \rho_A(\tau) \ \rho_G(\tau))^T$ . Here, for brevity, we have abbreviated the diagonal terms of the density matrix elements as  $\rho_I(\tau) = \rho_{II}(\tau)$ . The coefficient matrix  $\mathbf{U}(\eta, \lambda)$  can be expressed as

$$\mathbf{U}(\eta, \lambda) = \begin{pmatrix} \frac{\eta+1}{\eta} & -\frac{(\eta-1)(1+\lambda)}{2\eta} & -\frac{(\eta-1)(1-\lambda)}{2\eta} & 0 \\ -\frac{(\eta+1)(1+\lambda)}{2\eta} & 1+\lambda & 0 & -\frac{(\eta-1)(1+\lambda)}{2\eta} \\ -\frac{(\eta+1)(1-\lambda)}{2\eta} & 0 & 1-\lambda & -\frac{(\eta-1)(1-\lambda)}{2\eta} \\ 0 & -\frac{(\eta+1)(1+\lambda)}{2\eta} & -\frac{(\eta+1)(1-\lambda)}{2\eta} & \frac{\eta-1}{\eta} \end{pmatrix}, \quad (23)$$

Since  $\rho_G + \rho_E + \rho_A + \rho_S = 1$ , only three of the first four equations in Eq. (22) are independent. The general solution of Eq. (22) can be written in the following form

$$\begin{aligned}\mathbf{X}(\tau) &= \mathbf{M}_0(\eta) + \sum_{i=1}^3 \mathbf{M}_i(\rho(0), \eta, \lambda) [\Theta(\tau)]^{\xi_i}, \\ \rho_{IJ}(\tau) &= \rho_{IJ}(0) \Theta(\tau),\end{aligned}\quad (24)$$

where

$$\Theta(\tau) = e^{-\eta \Omega \Gamma_0 \tau}, \quad (25)$$

which ranges from 0 to 1, and it determines the entanglement evolution with time. Here,  $\xi_i(\eta, \lambda)$  and  $\mathbf{M}_i(\rho(0), \eta, \lambda)$  are respectively the eigenvalues and corresponding eigenvectors of the coefficient square matrix  $\mathbf{U}(\eta, \lambda)$ . The eigenvalues  $\xi_i$  satisfy the following equation,

$$\xi[\xi^3 - 4\xi^2 + (5 + \lambda^2 \eta^{-2} - 2\lambda^2)\xi - 2(1 - \lambda^2)] = 0. \quad (26)$$

Obviously, there is a definite zero root which we label as  $\xi_0 = 0$ , and the corresponding eigenvector  $\mathbf{M}_0(\eta)$  can be obtained as

$$\mathbf{M}_0(\eta) = \begin{pmatrix} (\eta + 1)^2 & \frac{\eta^2 - 1}{4\eta^2} & \frac{\eta^2 - 1}{4\eta^2} & \frac{(\eta - 1)^2}{4\eta^2} \end{pmatrix}^T. \quad (27)$$

The other three roots are labeled as  $\xi_1$ ,  $\xi_2$ ,  $\xi_3$ . Hereafter, the subscript “ $i$ ” of  $\xi_i$  runs from 1 to 3 except otherwise stated. Note that the analytical expressions for  $\xi_i(\eta, \lambda)$  and  $\mathbf{M}_i(\rho(0), \eta, \lambda)$  are shown in Appendix B.

We characterize the degree of entanglement by concurrence [48], which ranges from 0 for separable states, to 1 for maximally entangled states. For the X-type states, the concurrence takes the following form [28]

$$C[\rho(\tau)] = \max\{0, K_1(\tau), K_2(\tau)\}, \quad (28)$$

where

$$\begin{aligned}K_1(\tau) &= \sqrt{[\rho_A(\tau) - \rho_S(\tau)]^2 - [\rho_{AS}(\tau) - \rho_{SA}(\tau)]^2} - 2\sqrt{\rho_G(\tau)\rho_E(\tau)}, \\ K_2(\tau) &= 2|\rho_{GE}(\tau)| - \sqrt{[\rho_A(\tau) + \rho_S(\tau)]^2 - [\rho_{AS}(\tau) + \rho_{SA}(\tau)]^2}.\end{aligned}\quad (29)$$

Substituting Eq. (24) into Eq. (28), one can obtain the concurrence  $C$ , which can be formally written as  $C[\Omega\tau, \rho(0), \eta, \lambda]$ .

### III. ENTANGLEMENT DYNAMICS OF A UNIFORMLY ACCELERATED QUANTUM SYSTEM COUPLED WITH MASSIVE SCALAR FIELDS

In this section, we study the entanglement dynamics of a quantum system composed of two uniformly accelerated Unruh-DeWitt detectors coupled with massive scalar fields in the Minkowski vacuum. With the help of the parameters  $\{\Omega, \eta, \lambda\}$  defined in the previous section, we discuss the influences of the mass of the field and the acceleration on the entanglement dynamics. In particular, we focus on the time-delay, entanglement degradation, entanglement generation, and the anti-Unruh effect in entanglement evolution.

#### A. The time-delay effect

From the time evolution of the density matrix Eqs. (24) and (25), it is obvious that the factor  $\Omega$  plays the role of delaying the entanglement evolution, since its range is  $0 \leq \Omega \leq 1$ . This time-delay effect of the entanglement evolution is general, which is independent of the initial state of the system, or the feature of entanglement evolution (e.g. entanglement generation, degradation, revival, etc). That is, the evolution time for the quantum system coupled with massive fields is always  $\Omega^{-1}$  times that of the massless case.

For uniformly accelerated Unruh-DeWitt detectors coupled to massive scalar fields, the factor  $\Omega_a$  can be written as a function of  $m/\omega$  and  $a/\omega$ , whose analytical expression and the numerical values are shown in Eq. (12) and Fig. 1 respectively. In Ref. [38], the properties of  $\Omega_a(m/\omega, a/\omega)$  have been studied in detail. The properties of  $\Omega_a$  under some limiting conditions, such as the low and high acceleration limit, and the low and high mass limit, are shown in Appendix C. In the following, we analyze the influences of the mass of the field and the acceleration on the time-delay effect in entanglement evolution.

##### 1. The mass effects

In this part, we focus on the effects of mass on the time-delay effect. Compared with the massless case, the entanglement evolution in the massive case is generally slower since  $\Omega_a \leq 1$ . When  $m \rightarrow 0$ ,  $\Omega_a$  tends to that in the massless case, i.e.,  $\Omega_{0a} = 1$ . Also, it can be proved that  $d\Omega_a/dm \leq 0$  (See Eq. (C2) in Appendix C), so the larger the mass  $m$ , the slower the evolution. Especially, when  $m/\omega \geq 1$ , the time delay will increase exponentially.

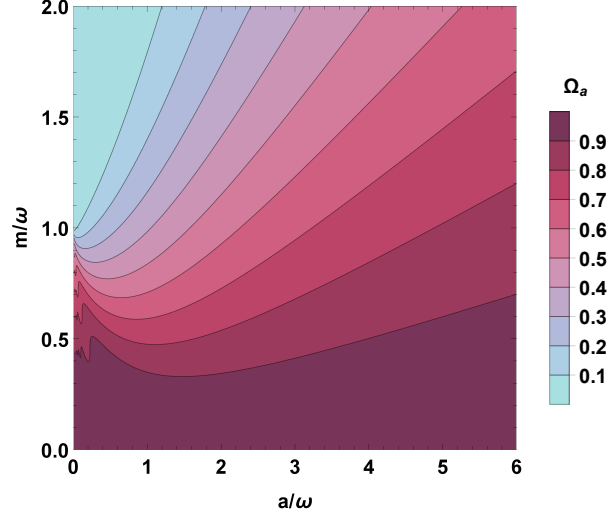


FIG. 1: The contour map of the factor  $\Omega_a$  in parameter space  $(a/\omega, m/\omega)$ .

(See Appendix C for the details of the properties of  $\Omega_a$ .) This time-delay phenomenon is shown in Fig. 2.

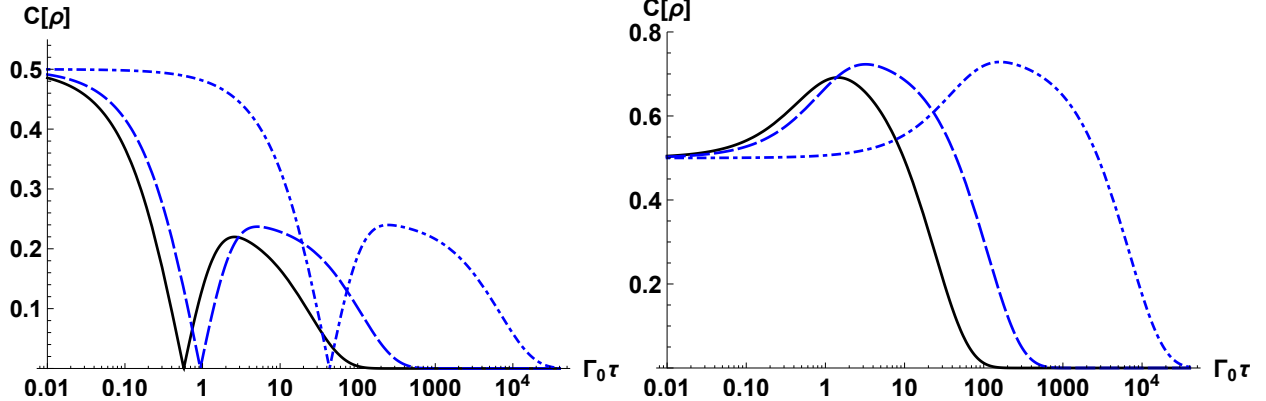


FIG. 2: Comparison between the dynamics of concurrence for uniformly accelerated quantum systems coupled with massive scalar fields (blue lines) and massless scalar fields (black lines) initially prepared in  $\frac{1}{2}|A\rangle + \frac{\sqrt{3}}{2}|S\rangle$  (left) and  $\frac{\sqrt{3}}{2}|A\rangle + \frac{1}{2}|S\rangle$  (right), with  $\omega L = 0.5$ ,  $a/\omega = 0.1$ . The black solid, blue dashed and dot-dashed lines correspond to  $m/\omega = 0, 0.8, 1.2$  respectively.

## 2. The acceleration effects

Comparing  $\Omega_a$  and  $\Omega_\beta$  given in Eqs. (12) and (13), one finds that, for uniformly accelerated Unruh-DeWitt detectors in the Minkowski vacuum,  $\Omega_a$  is not only related to the field

mass  $m/\omega$ , but also to the acceleration  $a/\omega$ . However, for the static ones in a thermal bath,  $\Omega_\beta$  is only related to  $m/\omega$  but not to the temperature of the bath  $T_U$  [41]. This leads to significant differences between the two cases.

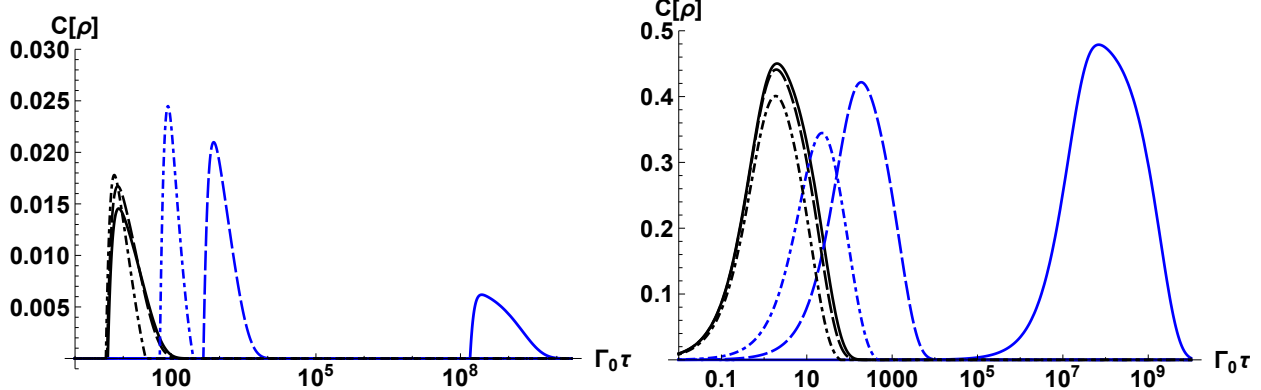


FIG. 3: Comparison between the dynamics of concurrence for uniformly accelerated quantum systems coupled with massive scalar fields (blue lines,  $m/\omega = 2$ ) and massless scalar fields (black lines,  $m/\omega = 0$ ) initially prepared in  $|E\rangle$  (left) and  $\frac{\sqrt{2}}{2}|A\rangle \pm \frac{\sqrt{2}}{2}|S\rangle$  (i.e.  $|10\rangle$  or  $|01\rangle$ ) (right), with  $\omega L = 0.5$ . The solid, dashed and dot-dashed lines correspond to  $a/\omega = 0.1, 0.5, 1$  respectively.

Firstly, as shown in Fig. 1, when  $m < \omega$ , the factor  $\Omega_a$  oscillates as the acceleration increases when the acceleration is small, and increases monotonically with the acceleration when the acceleration is large enough. When  $m \geq \omega$ , the factor  $\Omega_a$  increases monotonically with the acceleration. In either case,  $\Omega_a \rightarrow 1$  when the acceleration tends to infinity (See Appendix C for the proof). That is, the time-delay effect brought by field being massive can be counteracted by a large enough acceleration (See also Fig. 3). This is in sharp contrast to the case of a static quantum system in a thermal bath, where this time delay brought by the field being massive is not affected by the temperature. Secondly, in the thermal case, when  $m/\omega \geq 1$ ,  $\Omega_\beta = 0$ , which means that the quantum system is locked up in its initial state  $\rho(\tau) = \rho(0)$ , and the concurrence is a constant [41]. However, in the acceleration case, as long as  $a \neq 0$ ,  $\Omega_a \neq 0$ , and so the entanglement still evolves, although the evolution may be very slow because  $\Omega_a \rightarrow 0$  when  $a \rightarrow 0$ .

## B. The entanglement degradation effect

The entanglement degradation effect can be characterized by the factor  $\eta = \coth[\omega/(2T_K)]$  defined in Eq. (15), where  $T_K$  is the Unruh temperature in the acceleration case and is the environment temperature in the thermal case. We discuss the entanglement degradation effect brought by  $\eta$  from the following three aspects.

Firstly, the larger the factor  $\eta$ , the smaller the asymptotic entanglement of the quantum system. When the separation between the two detectors is nonvanishing, according to Eq. (24), we can get

$$K_1(\infty) = K_2(\infty) = \frac{1}{2}(\eta^{-2} - 1) \leq 0, \quad (30)$$

so  $C(\infty) = 0$ , which indicates that the final state is a separable state. When the separation between the two detectors is vanishing,  $\lambda = 1$ . From the general solution (24), we can obtain

$$\begin{aligned} K_1(\infty) &= \frac{|4\eta^2\rho_A(0) + 1 - \eta^2| - 2(\eta^2 - 1)(1 - \rho_A(0))}{3\eta^2 + 1}, \\ K_2(\infty) &= -\frac{2(\eta^2 + 1)\rho_A(0) + \eta^2 - 1}{3\eta^2 + 1} \leq 0. \end{aligned} \quad (31)$$

In this case,  $C(\infty)$  is related to the initial state  $\rho_A(0)$ , and the final state is entangled when  $\rho_A(0) > \frac{3(\eta^2 - 1)}{2(3\eta^2 - 1)} = \rho_A(0)_{crit}$ . In either case, it is easy to prove that  $\frac{dK_1(\infty)}{d\eta} \leq 0$ ,  $\frac{dK_2(\infty)}{d\eta} \leq 0$ , which indicates that  $\eta$  plays the role of entanglement degradation.

Secondly,  $\eta$  appears in  $\Theta(\tau) = e^{-\eta\Omega\Gamma_0\tau}$ , which shows that it accelerates the evolution of the system. In other words, it speeds up the disentanglement of a quantum system when there is a finite separation between the two detectors.

Thirdly,  $\eta$  also affects the value of the eigenvector  $\mathbf{M}_i(\rho(0), \eta, \lambda, \gamma)$  (i.e., the amplitude functions in Eq. (24)) and the eigenvalues  $\xi_i(\eta, \lambda, \gamma)$  of the coefficient matrix  $\mathbf{U}(\eta, \lambda)$ , which affect the phenomena of entanglement evolution, such as entanglement creation, revival, enhancement, etc. We show the effect of  $\eta$  on the concurrence coefficients  $K_1$  and  $K_2$  defined in Eq. (29) in Fig. 4. There one can see that the larger the  $\eta$  (the temperature  $T_K$ ), the more the curve of  $K_{1(2)}$  moves downwards, and the smaller the concurrence is. So the phenomena of entanglement generation, enhancement, and revival will not shown up when the factor  $\eta$  becomes large enough.

To summarize, the factor  $\eta$ , which describes the thermal dissipative effect of the environment, plays the role of degrading entanglement in entanglement dynamics. It is only related

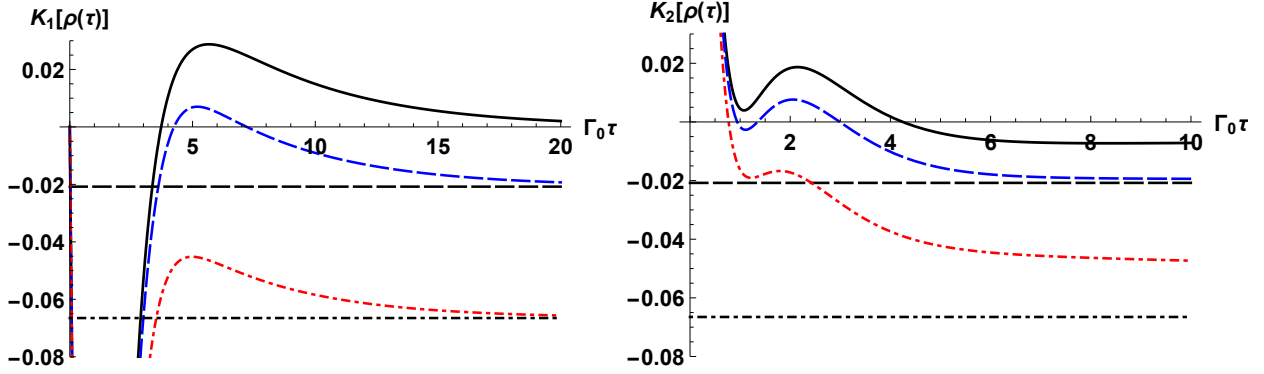


FIG. 4: The time evolution of the concurrence parameters  $K_1$  (left, with  $\lambda = 0.8, \gamma = 0.2$ ) and  $K_2$  (right, with  $\lambda = 0.98, \gamma = 0$ ) with different dissipation factor  $\eta = \coth[\omega/(2T_K)]$ , for two-atom system prepared in  $\sqrt{0.13}|g\rangle + \sqrt{0.87}|e\rangle$ , with  $\theta = 0$ . The black solid (horizontal axis), blue (black) dashed and red (black) dot-dashed lines are the evolution-lines (asymptotes) corresponding to  $T_K/\omega = 0, 0.20, 0.30$  respectively.

to the Unruh temperature in the acceleration case and the environment temperature in the thermal case.

### C. The entanglement generation effect

The entanglement generation effect is crucially dependent on the factor  $\lambda$  ( $|\lambda| \leq 1$ ) defined in Eq. (17). In fact, a large enough  $|\lambda|$  is a necessary condition for entanglement generation. When  $\lambda = 0$ , it can be proved that  $dC(\tau)/d\tau \leq 0$  (See Appendix D). That is, it is impossible to create entanglement if the system is initially separable when  $\lambda = 0$ .

In the following, we investigate the entanglement generation of a quantum system with the initial state  $|E\rangle$ . We focus on the relationship between entanglement creation and the factor  $\lambda$ . In Fig. 5, we show the maximum of concurrence  $C_{max}$  during evolution in the parameter space  $(\lambda, 2\pi T_K/\omega)$ . Here only the  $\lambda > 0$  part is shown, because it is symmetric about  $\lambda = 0$ . When  $\lambda = 0$ , entanglement cannot be generated, and when  $\lambda = 1$ , entanglement can neither be generated. The range of  $\lambda \in (\lambda_{min}, \lambda_{max})$  within which entanglement can be created is related to the value of the temperature  $T_K$ .

For a quantum system composed of two uniformly accelerated Unruh-DeWitt detectors coupled with massive scalar field in the Minkowski vacuum, the coherence factor  $\lambda_a$  can

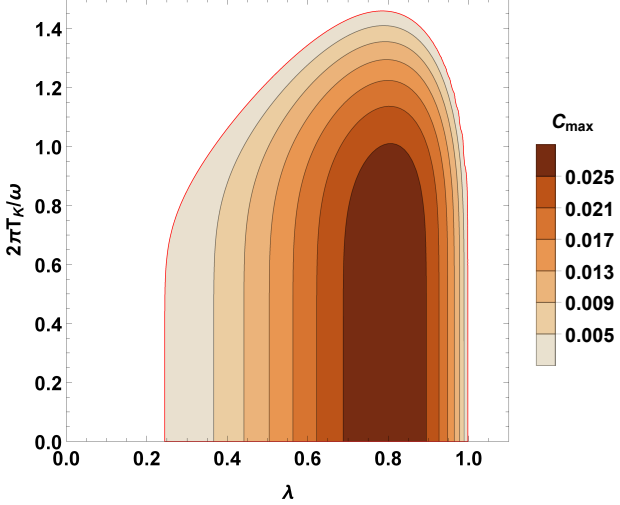


FIG. 5: The contour map of the maximum of concurrence during evolution  $C_{max}$  for quantum systems initially prepared in  $|E\rangle$ . Note that contour lines with  $C_{max} < 0.001$  are not drawn here.

be written as  $\lambda_a(m/\omega, a/\omega, \omega L)$ , whose explicit expression has been given in Eq. (19), and the expressions in several limiting cases have been shown in Appendix E. Now, we focus on how the mass of the field and the acceleration affect the parameter regions within which the system can get entangled.

### 1. The mass effects

In this part, we study the parameter regions within which entanglement creation can occur for two uniformly accelerated Unruh-DeWitt detectors prepared in  $|E\rangle$  coupled with massive scalar fields, and compare the result with that in the massless case. We examine two situations, namely  $m \geq \omega$  (Fig. 6) and  $m < \omega$  (Fig. 7).

Firstly, in Figs. 6 and 7, it is shown that, compared with the massless case, the region of separation  $\omega L$  within which entanglement can be created is expanded when the acceleration  $a/\omega$  is smaller than a critical value  $a_{crit}/\omega$  determined by the field mass  $m/\omega$ , and is compressed when  $a > a_{crit}$ . This is distinct from the fact that the region of separation for entanglement generation is always expanded for a static quantum system coupled with massive fields (in vacuum or in a thermal bath), compared with the massless case [41].

Secondly, by comparing Fig. 6 and Fig. 7, we find that the behaviors of the factor  $\lambda_a$  at  $a \rightarrow 0$  is completely different for  $m < \omega$  and  $m > \omega$ , resulting in a significant difference in the

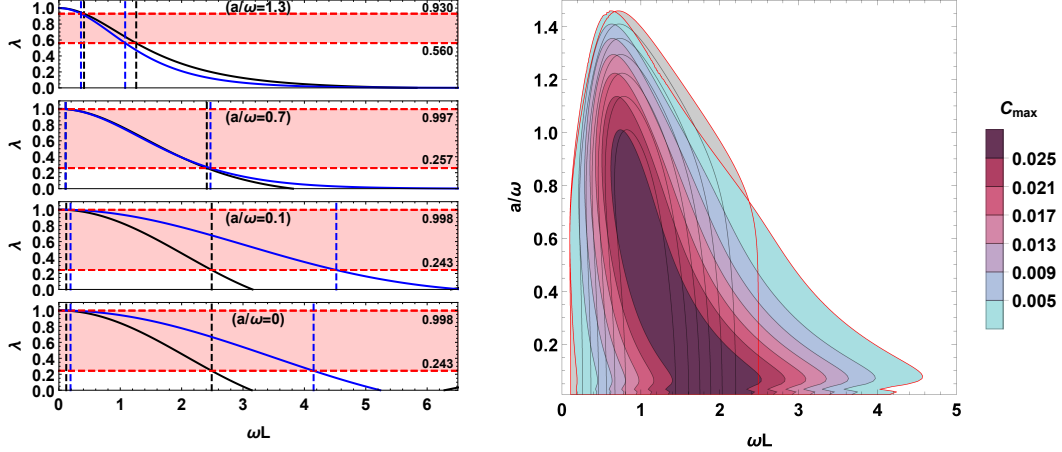


FIG. 6: (Left) The factor  $\lambda$  as a function of separation  $\omega L$ , with different accelerations  $a/\omega$ . The red dotted lines mark the upper and lower limits  $\lambda_{max}$  and  $\lambda_{min}$  within which entanglement can be generated ( $C_{max} \geq 0.001$ ). (Right) Contour map of the maximal concurrence during evolution for quantum systems prepared in  $|E\rangle$  in the parameter space  $(\omega L, a/\omega)$ . The figures show the differences between the results in the massive case ( $m/\omega = 0.8$ , the blue lines on the left, and the colored contour on the right) and the massless case (the black lines on the left, and the un-colored contour on the right).

possible regions of separation  $\omega L$  for entanglement creation. In the acceleration case, when the mass of the field exceeds the energy level spacing of the Unruh-DeWitt detectors, long-distance entanglement creation can be achieved when the acceleration is small, in contrast to the static case in which the mass of the field has to be smaller than but close to the energy level spacing in order to achieve long-distance entanglement [41].

## 2. The acceleration effects

Now we focus on the effects of acceleration on entanglement evolution, and compare the results with those of static ones in a thermal bath at the Unruh temperature. First, according to the analytical expressions Eqs. (19) to (20), in the acceleration case, the factor  $\lambda_a$  is a function of the acceleration  $a$ , while in the thermal case,  $\lambda_\beta$  is independent of temperature, which results in essential differences between the two cases.

In Fig. 8, it is shown that when  $a/\omega = 0$ , the acceleration case is the same as the static case as expected. When the acceleration increases, in a certain region where the acceleration

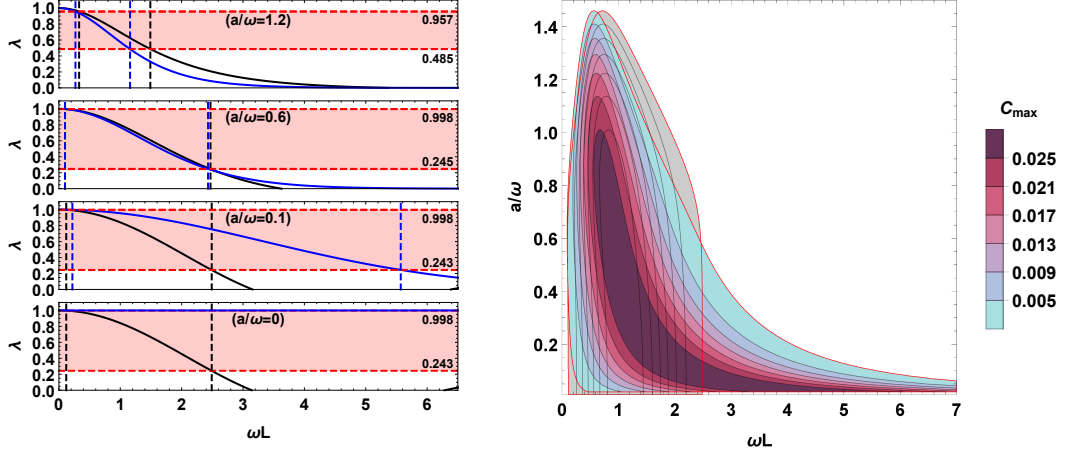


FIG. 7: (Left) The factor  $\lambda$  as a function of separation  $\omega L$ , with different accelerations  $a/\omega$ . The red dotted lines mark the upper and lower limits  $\lambda_{max}$  and  $\lambda_{min}$  within which entanglement can be generated ( $C_{max} \geq 0.001$ ). (Right) Contour map of the maximal concurrence during evolution for quantum systems prepared in  $|E\rangle$  in the parameter space  $(\omega L, a/\omega)$ . The figures show the differences between the results in the massive case ( $m/\omega = 1.2$ , the blue lines on the left, and the colored contour on the right) and the massless case (the black lines on the left, and the un-colored contour on the right).

is relatively small, the possible region of separation  $\omega L$  for entanglement generation varies oscillatorily from being compressed to being enlarged compared with that in the thermal case, due to the oscillation of  $\lambda_a$  with acceleration  $a$ . The amplitude of this oscillation increases with acceleration, until the maximal amplitude is reached (at about  $a/\omega \approx 0.1$  in Fig. 8), which causes a maximal expansion of the possible region of separation  $\omega L$  for entanglement generation. Then,  $\lambda_a$  decays monotonically with acceleration, which causes the compression of the possible region of separation  $\omega L$  for entanglement generation compared with that of the thermal case, as shown in Fig. 8. However, in the thermal case, since  $\lambda_\beta$  is independent of temperature, the possible region of separation  $\omega L$  for entanglement generation decreases monotonically as temperature increases.

In Fig. 9, we study the effects of mass on entanglement dynamics for two uniformly accelerated Unruh-DeWitt detectors, and compare the results with those of in the thermal case. From Fig. 9, we draw the following conclusions<sup>1</sup>:

<sup>1</sup> In Fig. 9, the acceleration is set to  $a/\omega = 0.1$ . However, the conclusions still hold if a larger acceleration

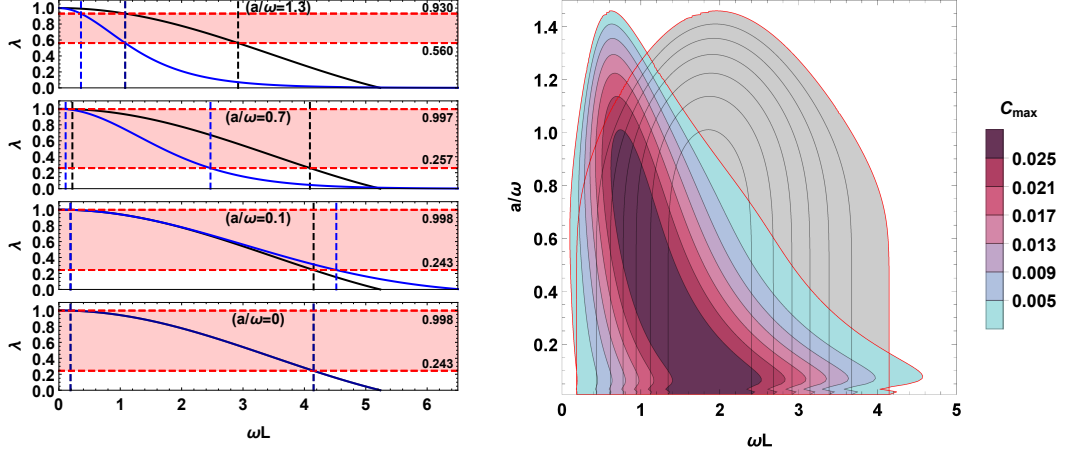


FIG. 8: (Left) The factor  $\lambda$  as a function of separation  $\omega L$ , with different accelerations  $a/\omega$ . The red dotted lines mark the upper and lower limits  $\lambda_{max}$  and  $\lambda_{min}$  within which entanglement can be generated ( $C_{max} \geq 0.001$ ). (Right) Contour map of the maximal concurrence during evolution for quantum systems prepared in  $|E\rangle$  with  $m/\omega = 0.8$  in the parameter space  $(\omega L, a/\omega)$ . The figures show the differences between the results in the acceleration case (the blue lines on the left, and the colored contour on the right) and the thermal case (the black lines on the left, and the un-colored contour on the right).

1) When  $m/\omega < 1$ , in the thermal case, the damping of  $\lambda_\beta$  with  $\omega L$  gradually slows down as  $m/\omega$  increases. When  $m/\omega \rightarrow 1$ ,  $\lambda_\beta$  becomes a constant ( $\lambda_\beta = 1$ ). As a result, the region of  $\omega L$  within which entanglement can be generated is significantly enlarged when  $m/\omega$  is close to 1. However, in the acceleration case,  $\lambda_a$  does not approach a constant no matter how large the mass is. Therefore, the regions of  $\omega L$  within which the two detectors can be entangled are only slightly enlarged.

2) When  $m/\omega \geq 1$ , there are significant differences between the acceleration case and the thermal case. For the thermal case, the factor  $\Omega_\beta$  equals to 0, so the detectors are locked up in the initial state as if it were a closed system, and entanglement generation cannot occur. However, in the acceleration case, no matter how large  $m/\omega$  is (as long as it is not infinite, see Eq. (E3)),  $\lambda_a$  is a function of  $\omega L$  ranging from 0 to 1, and the factor  $\Omega_a \neq 0$ . Therefore, entanglement generation is possible for certain  $\omega L$  (but it may take a long time since the factor  $\Omega_a$  decays exponentially as  $m/\omega$  increases).

---

is chosen.

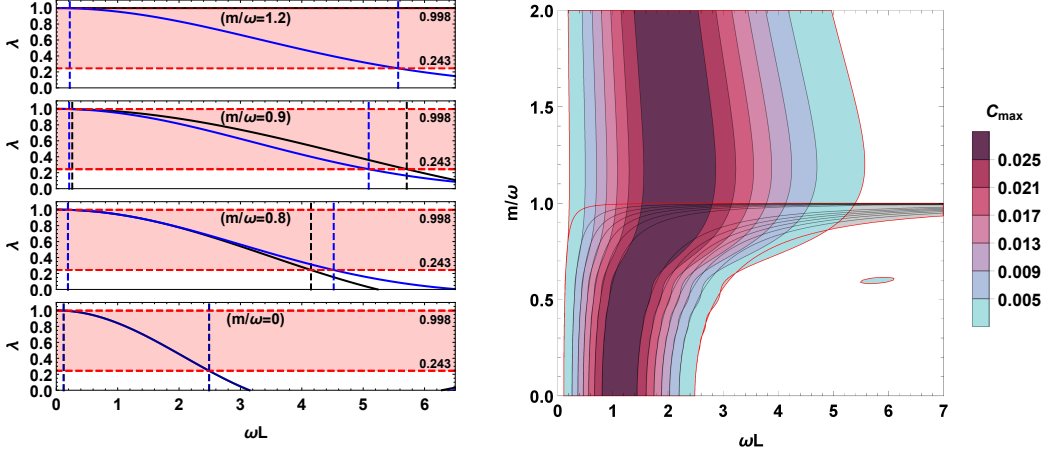


FIG. 9: (Left) The factor  $\lambda$  as a function of separation  $\omega L$ , with different mass  $m/\omega$ . The red dotted lines mark the upper and lower limits  $\lambda_{max}$  and  $\lambda_{min}$  within which entanglement can be generated ( $C_{max} \geq 0.001$ ). (Right) Contour map of the maximal concurrence during evolution for quantum systems prepared in  $|E\rangle$  with  $a/\omega = 0.1$  in the parameter space  $(\omega L, m/\omega)$ . The figures show the differences between the results in the acceleration case (the blue lines on the left, and the colored contour on the right) and the thermal case (the black lines on the left, and the un-colored contour on the right).

#### D. The anti-Unruh effect

The Unruh effect can be sensed by a quantum system coupled with the vacuum fields, i.e. an Unruh-DeWitt detector [3, 5]. For static detectors in a thermal bath, it is well-known that the higher the temperature, the more often the detector clicks. Since the Unruh temperature is proportional to the proper acceleration [3], it is expected the larger the acceleration, the more often the Unruh-DeWitt detector clicks. However, in certain cases, the transition rate of a uniformly accelerated detector may decrease with acceleration in some parameter regimes, e.g. in the presence of a boundary [8], when the field the detector coupled with is massive [38], and when the duration of the detector-field coupling is finite [39] (but long enough to satisfy the KMS condition [44–46]). This phenomenon is named as the anti-Unruh effect in Ref. [39], and is further divided into two categories [40], i.e. the strong anti-Unruh effect (the effective excitation-to-deexcitation ratio (EDR) temperature of a detector decreases as the KMS temperature increases), and the weak anti-Unruh effect (a detector clicks less often as the KMS temperature increases), which is a necessary condition

for the strong one. Recently, it is found that the anti-Unruh effect introduced in Refs. [39, 40] may possibly be viewed as an amplification mechanism for quantum entanglement within a certain parameter regime [49].

In Ref. [34], we have shown that, for a pair of two-level detectors coupled with massless scalar fields, the maximal concurrence during evolution may increase with acceleration for specific inter-detector separations, in contrast to the fact that it always decreases monotonically with temperature in the thermal case. This may also be called an anti-Unruh phenomenon in terms of the entanglement generated. In the massive case, as shown in the contour maps (Figs. 6 and 7), for any inter-detector separation, the maximal concurrence quantifying the entanglement generated during evolution may increase with acceleration when the acceleration is relatively small with respect to the energy level spacing of the detectors. Therefore, in contrast to the massless case in which the anti-Unruh phenomenon appears only for specific separation, it is a general phenomenon in the massive case.

As an example, in Fig. 10, we plot the maximal concurrence as a function of acceleration  $a/\omega$  with fixed mass  $m/\omega$  and separation  $\omega L$ . As shown in Fig. 10 (left), when  $m/\omega < 1$ , for small accelerations ( $a/\omega < 0.58$ ), the maximal concurrence oscillates with acceleration since the entanglement creation effect from  $\lambda$  which oscillates with acceleration is stronger than the entanglement degradation effect from  $\eta$ . However, when the acceleration is large enough ( $a/\omega > 0.58$ ), the maximal concurrence decreases monotonically with acceleration. When  $m/\omega > 1$ , since  $\lambda$  decays monotonically with acceleration from 1 (when  $a/\omega = 0$ ) to 0 (when  $a/\omega \rightarrow \infty$ ), the maximal concurrence varies from 0 (when  $a/\omega = 0$ ) to a certain non-zero maximum value (when  $a/\omega = 0.22$ ), and then to 0 (when  $a/\omega > 1.04$ ), as shown in Fig. 10 (right). In either case, the anti-Unruh phenomenon occurs when the acceleration is relatively small with respect to the energy level spacing of the detectors ( $a/\omega < 0.58$  in the first case, and  $a/\omega < 0.22$  in the second case).

Based on the previous discussions, the emergence of the anti-Unruh phenomenon in terms of entanglement generated can be understood as follows. The factor  $\eta$  always hinders entanglement generation. The larger the  $\eta$ , the less easily the entanglement generation occurs. On the other hand, the factor  $\lambda$  is conducive to entanglement generation. In the thermal case, the factor  $\lambda_\beta$  is independent of temperature, so the environment temperature determines the factor  $\eta$  only, which gives rise to a degradation effect on entanglement evolution. However, in the acceleration case, the factor  $\lambda_a$  is related to the acceleration, so the acceleration

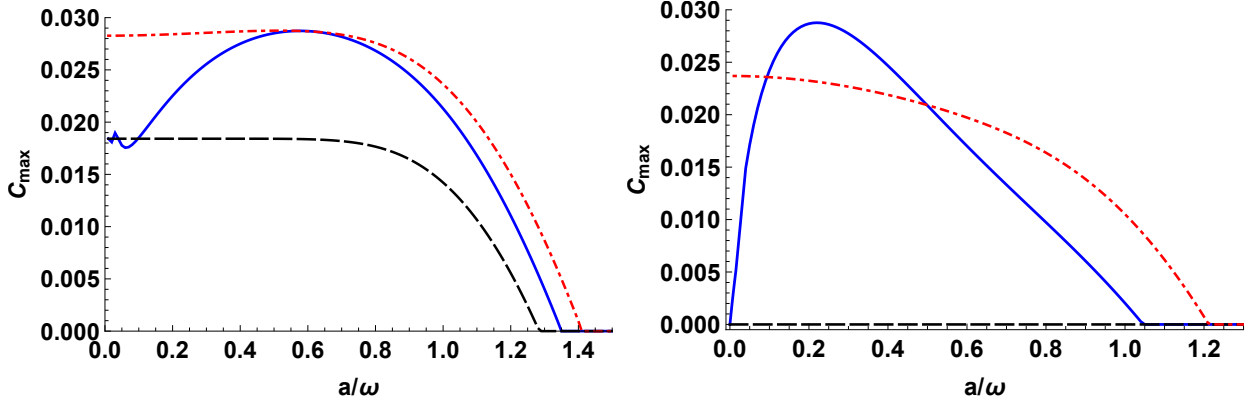


FIG. 10: Comparison between the maximum of concurrence during evolution for uniformly accelerated quantum systems coupled with massive (blue solid lines) and massless (red dot-dashed lines), and static ones coupled with massive scalar fields in a thermal bath at the Unruh temperature (black dashed lines) initially prepared in  $|E\rangle$ . Here,  $m/\omega = 0.8$ ,  $\omega L = 1.0$  (left), and  $m/\omega = 1.2$ ,  $\omega L = 1.5$  (right).

contributes not only to the degradation effect, but also to the entanglement creation effect. When the entanglement creation effect overweighs the dissipation effect, the anti-Unruh phenomenon appears.

#### IV. SUMMARY

In this paper, we have investigated, in the framework of open quantum systems, the entanglement dynamics of a quantum system composed of two uniformly accelerated Unruh-DeWitt detectors coupled with fluctuating massive scalar fields in the Minkowski vacuum. We obtain the general solution to the master equation describing the evolution of the system, and calculate the concurrence as a measure of the entanglement of the quantum system. We focus on the effects of field mass and acceleration on the entanglement dynamics, and find that the entanglement dynamics for uniformly accelerated detectors coupled with massive fields is essentially different from that of the static ones in a thermal bath at the Unruh temperature. The details follow.

Firstly, the entanglement evolution process for a quantum system coupled with massive fields is always slower compared with that of the one coupled with massless fields, and this time-delay effect brought by the field being massive can however be counteracted by a

large enough acceleration. It is interesting to note, however, that in the thermal case, this time delay is not affected by the temperature. In particular, when the mass of the field is greater than the energy level spacing of the detectors, static detectors in a thermal bath will be locked up in its initial state, while entanglement generation is still possible in the acceleration case.

Secondly, the region of spatial separation between the detectors within which entanglement can be generated is always enlarged for a static quantum system coupled with massive fields in a thermal bath compared with that in the massless case, while it can be both compressed and enlarged in the acceleration case.

Thirdly, the maximal concurrence of the quantum system generated during evolution may increase with acceleration when the acceleration is relatively small compared with the energy level spacing of the detectors for any inter-detector separation, in contrast to the monotonic decreases of the maximal concurrence with temperature for static detectors in a thermal bath, which can be considered as an anti-Unruh effect in terms of the entanglement generated.

### Acknowledgments

This work was supported in part by the NSFC under Grants No. 11805063, No. 11690034, and No. 12075084, and the Hunan Provincial Natural Science Foundation of China under Grant No. 2020JJ3026.

### Appendix A: The expressions of the entanglement dynamic parameters in various cases

In the free Minkowski spacetime, the field operator  $\phi(t, \mathbf{x})$  for a massive scalar field can be expanded as

$$\phi(t, \mathbf{x}) = \int d^3k \frac{1}{\sqrt{2\omega_k(2\pi^3)}} [a_k e^{i\mathbf{k}\mathbf{x} - i\omega_k t} + a_k^\dagger e^{-i\mathbf{k}\mathbf{x} + i\omega_k t}], \quad (\text{A1})$$

where  $a_k$  and  $a_k^\dagger$  are the annihilation and creation operators for field quanta with frequency  $\omega_k$  and momentum  $k = |\mathbf{k}|$  satisfying the dispersion relation  $\omega_k^2 = k^2 + m^2$ , with  $m$  being

mass of the scalar fields. Substituting Eq. (A1) into Eq. (7), we obtain

$$\begin{aligned} C^{(\alpha\varrho)}(\Delta\tau) &= \frac{1}{4\pi^2} \int_m^\infty (2\langle N_{\omega_k} \rangle + 1) \frac{\sin(\sqrt{\omega_k^2 - m^2} |\Delta\vec{x}_{\alpha\varrho}|)}{|\Delta\vec{x}_{\alpha\varrho}|} \cos(\omega_k \Delta t_{\alpha\varrho}) d\omega_k, \\ \chi^{(\alpha\varrho)}(\Delta\tau) &= \frac{-i}{4\pi^2} \int_m^\infty \frac{\sin(\sqrt{\omega_k^2 - m^2} |\Delta\vec{x}_{\alpha\varrho}|)}{|\Delta\vec{x}_{\alpha\varrho}|} \sin(\omega_k \Delta t_{\alpha\varrho}) d\omega_k, \end{aligned} \quad (\text{A2})$$

where  $|\Delta\vec{x}_{\alpha\varrho}| = \sqrt{(x_\alpha - x'_\varrho)^2 + (y_\alpha - y'_\varrho)^2 + (z_\alpha - z'_\varrho)^2}$ ,  $\Delta t_{\alpha\varrho} = t_\alpha - t'_\varrho$ , and  $N_{\omega_k} = a_k^\dagger a_k$  is the particle number operator.

### 1. The acceleration case

For a uniformly accelerated quantum system composed of two Unruh-DeWitt detectors with a separation perpendicular to the acceleration, the trajectories of each detector are

$$\begin{aligned} t_1(\tau) &= \frac{1}{a} \sinh a\tau, \quad x_1(\tau) = \frac{1}{a} \cosh a\tau, \quad y_1(\tau) = 0, \quad z_1(\tau) = 0, \\ t_2(\tau) &= \frac{1}{a} \sinh a\tau, \quad x_2(\tau) = \frac{1}{a} \cosh a\tau, \quad y_2(\tau) = 0, \quad z_2(\tau) = L. \end{aligned} \quad (\text{A3})$$

Substituting the trajectories above into Eqs. (A2) and (9), and using the following integral formulae

$$\begin{aligned} \int_{-\infty}^{+\infty} \cos[(2\omega_k/a) \sinh(au/2)] e^{i\omega u} du &= (4/a) \cosh(\pi\omega/a) K_{i2\omega/a}(2\omega_k/a), \\ \int_{-\infty}^{+\infty} \sin[(2\omega_k/a) \sinh(au/2)] e^{i\omega u} du &= (4i/a) \sinh(\pi\omega/a) K_{i2\omega/a}(2\omega_k/a), \end{aligned} \quad (\text{A4})$$

one obtains

$$\begin{aligned} \mathcal{F}_{C_a}^{(\alpha\varrho)}(\omega) &= \frac{\mu^2 \omega}{2\pi} \frac{4 \cosh(\pi\omega/a)}{\pi\omega/a} \int_{\frac{m}{a}}^\infty \frac{\sin(a|\Delta z_{\alpha\varrho}| \sqrt{x^2 - m^2/a^2})}{a|\Delta z_{\alpha\varrho}|} K_{i2\omega/a}(2x) dx, \\ \mathcal{F}_{\chi_a}^{(\alpha\varrho)}(\omega) &= \frac{\mu^2 \omega}{2\pi} \frac{4 \sinh(\pi\omega/a)}{\pi\omega/a} \int_{\frac{m}{a}}^\infty \frac{\sin(a|\Delta z_{\alpha\varrho}| \sqrt{x^2 - m^2/a^2})}{a|\Delta z_{\alpha\varrho}|} K_{i2\omega/a}(2x) dx. \end{aligned} \quad (\text{A5})$$

Here, the subscript “ $a$ ” denotes the acceleration case,  $|\Delta z_{\alpha\varrho}| = L$  when  $\alpha \neq \varrho$ , and  $|\Delta z_{\alpha\varrho}| = 0$  when  $\alpha = \varrho$ . According to the definitions of  $\Omega$ ,  $\eta$  and  $\lambda$ , which have been shown in Eqs. (11), (15) and (17) respectively, we can obtain that

$$\Omega_a = \frac{\sinh(\pi\omega/a)}{\pi\omega/a} \frac{m^2}{a^2} [K_{1+i\omega/a}(m/a) K_{-1+i\omega/a}(m/a) - K_{i\omega/a}^2(m/a)], \quad (\text{A6})$$

$$\eta_a = \coth \frac{\pi \omega}{a} \quad (A7)$$

$$\lambda_a = \frac{4a^2}{m^2} \frac{\int_{\frac{m}{a}}^{\infty} \frac{1}{aL} \sin(aL\sqrt{x^2 - m^2/a^2}) K_{i2\omega/a}(2x) dx}{K_{1+i\omega/a}(m/a) K_{-1+i\omega/a}(m/a) - K_{i\omega/a}^2(m/a)}, \quad (A8)$$

## 2. The thermal bath case

For two static Unruh-DeWitt detectors in a thermal bath at temperature  $T = \frac{1}{\beta}$ ,  $\langle N_{\omega_k} \rangle = 1/(e^{\frac{\pi\omega}{T}} - 1) = 1/(e^{\pi\beta\omega} - 1)$ . Plugging Eq. (A2) into Eq. (9), we obtain

$$\begin{aligned} \mathcal{F}_{C_\beta}^{(\alpha\varrho)}(\omega) &= \begin{cases} \frac{\mu^2\omega}{2\pi} \frac{\sin(\sqrt{\omega^2-m^2}|\Delta z_{\alpha\varrho}|)}{\omega|\Delta z_{\alpha\varrho}|} \coth \frac{\omega}{2T}, & \omega > m, \\ 0, & 0 \leq \omega \leq m, \end{cases} \\ \mathcal{F}_{\chi_\beta}^{(\alpha\varrho)}(\omega) &= \begin{cases} \frac{\mu^2\omega}{2\pi} \frac{\sin(\sqrt{\omega^2-m^2}|\Delta z_{\alpha\varrho}|)}{\omega|\Delta z_{\alpha\varrho}|}, & \omega > m, \\ 0, & 0 \leq \omega \leq m. \end{cases} \end{aligned} \quad (A9)$$

Here the subscript “ $\beta$ ” denotes the thermal bath case. Direct calculations show that

$$\Omega_\beta = \begin{cases} \sqrt{1 - \frac{m^2}{\omega^2}}, & \omega > m, \\ 0, & \omega \leq m. \end{cases}, \quad \eta_\beta = \coth \frac{\beta\omega}{2} = \coth \frac{\omega}{2T}, \quad \lambda_\beta = \frac{\sin(\omega L \Omega_\beta)}{\omega L \Omega_\beta}. \quad (A10)$$

## Appendix B: The general solution of the master equation

In order to investigate the entanglement dynamics, we need to solve the time evolution equations of the density matrix elements (22). One can get the general solution of the density matrix elements as,

$$\begin{aligned} \mathbf{X}(\tau) &= \mathbf{M}_0(\eta) + \sum_{i=1}^3 \mathbf{M}_i(\rho(0), \eta, \lambda) e^{-\xi_i \eta \Omega \Gamma_0 \tau}, \\ \rho_{IJ}(\tau) &= \rho_{IJ}(0) e^{-\eta \Omega \Gamma_0 \tau}. \end{aligned} \quad (B1)$$

Here,  $\xi_i(\eta, \lambda)$  and  $\mathbf{M}_i(\rho(0), \eta, \lambda)$  are respectively the eigenvalues and the corresponding eigenvectors of the coefficient matrix  $\mathbf{U}(\eta, \lambda)$  shown in Eq. (23). The equation that the eigenvalues  $\xi_i$  satisfy can be written as,

$$\xi[\xi^3 - 4\xi^2 + (5 + \lambda^2 \eta^{-2} - 2\lambda^2)\xi - 2(1 - \lambda^2)] = 0. \quad (B2)$$

Obviously, there is a definite zero root which we label as  $\xi_0 = 0$ , and the corresponding eigenvector  $\mathbf{M}_0(\eta)$  can be written as

$$\mathbf{M}_0(\eta) = \begin{pmatrix} (\eta-1)^2 & \eta^2-1 & \eta^2-1 & (\eta+1)^2 \\ \frac{(\eta-1)^2}{4\eta^2} & \frac{\eta^2-1}{4\eta^2} & \frac{\eta^2-1}{4\eta^2} & \frac{(\eta+1)^2}{4\eta^2} \end{pmatrix}^T. \quad (\text{B3})$$

With the help of the Vieta's theorem, the other three roots satisfy the following properties,

$$\begin{aligned} \xi_1 + \xi_2 + \xi_3 &= 4, & \xi_1 \xi_2 \xi_3 &= 2(1 - \lambda^2), \\ \xi_1 \xi_2 + \xi_2 \xi_3 + \xi_1 \xi_3 &= 5 + (\eta^{-2} - 2)\lambda^2. \end{aligned} \quad (\text{B4})$$

The explicit expressions of  $\xi_i$  can be written as

$$\begin{aligned} \xi_1 &= \frac{4}{3} - \frac{2}{3}\sqrt{1 + 3\lambda^2(2 - \eta^{-2})} \cos [\theta(\eta, \lambda)/3], \\ \xi_2 &= \frac{4}{3} + \frac{2}{3}\sqrt{1 + 3\lambda^2(2 - \eta^{-2})} \cos [(\theta(\eta, \lambda) + \pi)/3], \\ \xi_3 &= \frac{4}{3} + \frac{2}{3}\sqrt{1 + 3\lambda^2(2 - \eta^{-2})} \cos [(\theta(\eta, \lambda) - \pi)/3], \end{aligned} \quad (\text{B5})$$

where  $\theta(\eta, \lambda)$  can be expressed as an inverse cosine function related to  $\lambda$  and  $\eta$ ,

$$\theta(\eta, \lambda) = \arccos \left( \frac{9\lambda^2(2\eta^{-2} - 1) - 1}{(1 + 3\lambda^2(2 - \eta^{-2}))^{3/2}} \right).$$

Note that  $\theta(\eta, \lambda)$  varies from 0 when  $\lambda = 1$  and  $\eta = 1$ , to  $\pi$  when  $\lambda = 0$ . The ranges of  $\xi_i$  ( $i = 1, 2, 3$ ) are  $\xi_1 \in [0, 1]$ ,  $\xi_2 \in [1, 2]$ ,  $\xi_3 \in [2, 3]$ , and the corresponding eigenvector  $\mathbf{M}_i(\rho(0), \eta, \lambda)$  can be written as,

$$\mathbf{M}_i(\rho(0), \eta, \lambda) = \begin{pmatrix} Q_E & Q_S & Q_A & Q_G \end{pmatrix}^T, \quad (\text{B6})$$

where

$$\begin{aligned} Q_E &= \left[ (\eta-1)^2[\xi_i(1 + \lambda^2) + (\lambda^2 - 1)]\rho_G(0) + (\lambda-1)(\eta\xi_i - \eta + 1)(\xi_i - \lambda - 1)(\eta - 1) \right. \\ &\quad \times \rho_A(0) + (\eta + 1)[2\eta\xi_i^2 + \xi_i(\lambda^2\eta - 5\eta - \lambda^2 + 1) + (3\eta - 1)(1 - \lambda^2)]\rho_E(0) \\ &\quad \left. + (\lambda + 1)(1 - \eta)(\eta\xi_i - \eta + 1)(\xi_i + \lambda - 1)\rho_S(0) \right] / h(\xi_i, \eta, \lambda), \end{aligned} \quad (\text{B7})$$

$$\begin{aligned} Q_S &= \left[ (\lambda + 1)(1 - \eta)(\eta\xi_i - \eta - 1)(\xi_i + \lambda - 1)\rho_G(0) + (1 - \lambda^2)(\eta^2 - 1)(\xi_i - 1)\rho_A(0) \right. \\ &\quad + (\lambda + 1)[2\eta^2\xi_i^2 - \xi_i(1 + 5\eta^2 + \lambda - 3\lambda\eta^2) + (3\eta^2 + 1)(1 - \lambda)]\rho_S(0) \\ &\quad \left. - (\lambda + 1)(1 + \eta)(\eta\xi_i - \eta + 1)(\xi_i + \lambda - 1)\rho_E(0) \right] / h(\xi_i, \eta, \lambda), \end{aligned} \quad (\text{B8})$$

$$\begin{aligned}
Q_A = & \left[ (\lambda - 1)(\eta - 1)(\eta\xi_i - \eta - 1)(\xi_i - \lambda - 1)\rho_G(0) + (1 - \lambda)[2\eta^2\xi_i^2 \right. \\
& - \xi_i(1 + 5\eta^2 - \lambda + 3\lambda\eta^2) + (3\eta^2 + 1)(1 + \lambda)]\rho_A(0) + (\lambda^2 - 1)(\eta^2 - 1)(\xi_i - 1)\rho_S(0) \\
& \left. + (\lambda - 1)(1 + \eta)(\eta\xi_i - \eta + 1)(\xi_i - \lambda - 1)\rho_E(0) \right] / h(\xi_i, \eta, \lambda), \tag{B9}
\end{aligned}$$

$$\begin{aligned}
Q_G = & \left[ (\eta - 1)[2\eta\xi_i^2 + \xi_i(\lambda^2\eta - 5\eta + \lambda^2 - 1) + (3\eta + 1)(1 - \lambda^2)]\rho_G(0) + (\lambda - 1)(\eta + 1) \right. \\
& \times (\eta\xi_i - \eta - 1)(\xi_i - \lambda - 1)\rho_A(0) - (\lambda + 1)(\eta + 1)(\eta\xi_i - \eta - 1)(\xi_i + \lambda - 1)\rho_S(0) \\
& \left. + (\eta + 1)^2[\xi_i(1 + \lambda^2) + (\lambda^2 - 1)]\rho_E(0) \right] / h(\xi_i, \eta, \lambda). \tag{B10}
\end{aligned}$$

Here  $h(\xi_i, \eta, \lambda) = 4[2\eta^2\xi_i^2 - (5\eta^2 + \lambda^2 - 2\eta^2\lambda^2)\xi_i + 3(1 - \lambda^2)\eta^2]$ . In the following, we discuss two special cases, i.e.  $\lambda = 1$  and  $\lambda = 0$ .

When  $\lambda = 1$ , the characteristic roots  $\xi_i$  can be calculated as,

$$\xi_1 = 0, \quad \xi_2 = 2 - \sqrt{1 - \eta^{-2}}, \quad \xi_3 = 2 + \sqrt{1 - \eta^{-2}}. \tag{B11}$$

With the help of Eq. (B10), in the neighborhood of  $\lambda = 1$ ,  $\xi_1$  can be expressed as

$$\xi_1 = \frac{4\eta^2}{3\eta^2 + 1}(1 - \lambda) + O[(1 - \lambda)^2]. \tag{B12}$$

Substituting Eqs. (B11) and (B12) into the general solutions (B1), and taking the limit of  $\lambda \rightarrow 1$ , one can obtain the diagonal density matrix elements as (the off-diagonal ones are the same as those in Eq. (B1))

$$\mathbf{X}(\tau) = \mathbf{M}_0(\eta) + \lim_{\lambda \rightarrow 1} \mathbf{M}_1(\rho(0), \eta, \lambda) + \sum_{i=2}^3 \mathbf{M}_i(\rho(0), \eta, 1) e^{-\xi_i \eta \Omega \Gamma_0 \tau}. \tag{B13}$$

Here, the steady-state value of  $\mathbf{X}(\tau)$  when  $\tau \rightarrow \infty$  can be written as

$$\mathbf{X}(\infty) = \begin{pmatrix} \frac{(\eta-1)^2}{1+3\eta^2}(1 - \rho_A(0)) \\ \frac{\eta^2-1}{1+3\eta^2}(1 - \rho_A(0)) \\ \rho_A(0) \\ \frac{(\eta+1)^2}{1+3\eta^2}(1 - \rho_A(0)) \end{pmatrix}. \tag{B14}$$

The equation above shows that, in this case, the steady state of the system is related to its initial state.

When  $\lambda = 0$ , the characteristic equation (B2) has one single root and two multiple roots, i.e.  $\xi_1 = \xi_2 = 1$ ,  $\xi_3 = 2$ . With the help of Eq. (B10), in the neighborhood of  $\lambda = 0$ ,  $\xi_i$  can be expressed as

$$\xi_1 = 1 - \eta^{-1}\lambda + O[\lambda^2], \quad \xi_2 = 1 + \eta^{-1}\lambda + O[\lambda^2], \quad \xi_3 \approx 2 + O[\lambda^2]. \tag{B15}$$

Then, substituting Eq. (B15) into Eq. (B6) and taking the limit of  $\lambda \rightarrow 0$ , one can obtain

$$\mathbf{X}(\tau) = \mathbf{M}_0(\eta) + (\mathbf{M}_1 + \mathbf{M}_2) e^{-\eta\Omega\Gamma_0\tau} + \mathbf{M}_3 e^{-2\eta\Omega\Gamma_0\tau}, \quad (\text{B16})$$

and the off-diagonal ones are the same as those in Eq. (B1). Here,

$$\mathbf{M}_1 + \mathbf{M}_2 = \frac{1}{2\eta^2} \begin{pmatrix} (\eta - 1)[1 + \eta(\rho_E(0) - \rho_G(0))] \\ 1 + \eta(\rho_E(0) - \rho_G(0)) + \eta^2(\rho_S(0) - \rho_A(0)) \\ 1 + \eta(\rho_E(0) - \rho_G(0)) + \eta^2(\rho_A(0) - \rho_S(0)) \\ -(\eta + 1)[1 + \eta(\rho_E(0) - \rho_G(0))] \end{pmatrix}, \quad (\text{B17})$$

and

$$\mathbf{M}_3 = \frac{1}{2\eta^2} \begin{pmatrix} \eta[(\eta + 1)\rho_E(0) + (\eta - 1)\rho_G(0)] + \frac{1-\eta^2}{2} \\ -\eta[(\eta + 1)\rho_E(0) + (\eta - 1)\rho_G(0)] - \frac{1-\eta^2}{2} \\ -\eta[(\eta + 1)\rho_E(0) + (\eta - 1)\rho_G(0)] - \frac{1-\eta^2}{2} \\ \eta[(\eta + 1)\rho_E(0) + (\eta - 1)\rho_G(0)] + \frac{1-\eta^2}{2} \end{pmatrix}. \quad (\text{B18})$$

Note that,  $\rho_E(0) + \rho_S(0) + \rho_A(0) + \rho_G(0) = 1$  has been used in the derivation of Eqs. (B17) and (B18).

### Appendix C: The limit properties of $\Omega_a(m/\omega, a/\omega)$

The factor  $\Omega_a$  in Eq. (12) can be obtained as follows,

$$\begin{aligned} \Omega_a &= \frac{4 \sinh(\pi\omega/a)}{\pi\omega/a} \int_0^\infty \frac{k^2}{\sqrt{k^2 + m^2/a^2}} K_{i2\omega/a} \left( 2\sqrt{k^2 + m^2/a^2} \right) dk \\ &= \frac{2 \sinh(\pi\omega/a)}{\pi\omega/a} \int_0^\infty k K_{i\omega/a}^2 \left( \sqrt{k^2 + m^2/a^2} \right) dk \\ &= \frac{\sinh(\pi\omega/a)}{\pi\omega/a} \frac{m^2}{a^2} [K_{1+i\omega/a}(m/a) K_{-1+i\omega/a}(m/a) - K_{i\omega/a}^2(m/a)], \end{aligned} \quad (\text{C1})$$

which can be written as a function of dimensionless variables as  $\Omega_a(m/\omega, a/\omega)$ . Furthermore, it can be obtained that

$$\frac{d\Omega_a}{dm} = -\frac{2 \sinh(\pi\omega/a)}{\pi\omega/a} \frac{m}{a^2} K_{i\omega/a}^2(m/a) \leq 0. \quad (\text{C2})$$

In the following, we discuss the limit properties of  $\Omega_a(m/\omega, a/\omega)$ .

## 1. The low-mass limit

When  $m \ll \omega$  and  $m \ll a$ ,  $\Omega_a(m/\omega, a/\omega)$  can be approximated by,

$$\Omega_a(m/\omega, a/\omega) \approx 1 - \frac{m^2}{2\omega^2} \left[ 1 + \left( 1 + \frac{\omega^2}{a^2} \right)^{-\frac{1}{2}} \cos \left( 2\frac{\omega}{a} \ln \frac{m}{2a} - \varphi(\omega/a) \right) \right], \quad (C3)$$

where  $\varphi(\alpha)$  is an argument function defined as

$$\varphi(\alpha) = \arg[(1 + i\alpha)\Gamma^2(i\alpha)]. \quad (C4)$$

Note that  $\Gamma(z)$  is the Euler gamma function. This shows that the mass-dependent term gives a small correction which is negative. When the mass of the scalar field approaches 0,

$$\lim_{m \rightarrow 0} \Omega_a(m/\omega, a/\omega) = 1, \quad (C5)$$

and the result reduces to that in the massless case as expected.

## 2. The high-mass limit

When the mass of scalar field is much larger than the energy level spacing and the acceleration, i.e.  $m \gg \omega$  and  $m \gg a$ ,  $\Omega_a(m/\omega, a/\omega)$  can be approximated by,

$$\Omega_a(m/\omega, a/\omega) \approx e^{-2\frac{m}{a}} \frac{\sinh(\pi\omega/a)}{2\omega/a}. \quad (C6)$$

For a fixed acceleration, it exponentially approaches to zero as the mass of the field increases. Thus,

$$\lim_{m \rightarrow \infty} \Omega_a(m/\omega, a/\omega) = 0. \quad (C7)$$

## 3. The low-acceleration limit

In the low-acceleration limit, i.e. the acceleration is much smaller than the energy level spacing and the field mass,  $a \ll \omega$  and  $a \ll m$ ,  $\Omega_a(m/\omega, a/\omega)$  can be approximately written as (for a detailed derivation see Ref. [38])

$$\Omega_a(m/\omega, a/\omega) \approx \begin{cases} \sqrt{1 - (m/\omega)^2} \left[ 1 + \cos(2\eta_1\omega/a) \left( \frac{1}{72} + \psi \right) \frac{a}{\eta_1\omega} \right], & \omega > m, \\ \frac{1}{2} \sqrt{(m/\omega)^2 - 1} \left( \frac{25}{72} + \psi \right) \frac{a}{\eta_2\omega} e^{-2\eta_2\omega/a}, & \omega \leq m. \end{cases} \quad (C8)$$

Here,  $\eta_1$ ,  $\eta_2$  and  $\psi$  are positive, which are defined respectively as

$$\begin{aligned}\eta_1 &= \ln \frac{\omega + \sqrt{\omega^2 - m^2}}{m} - \sqrt{1 - (m/\omega)^2}, \\ \eta_2 &= \sqrt{(m/\omega)^2 - 1} - \arccos(\omega/m), \\ \psi &= (1/12)t^3\eta + (1/4)t\eta,\end{aligned}$$

where  $t = [1 - (m/\omega)^2]^{-1/2}$  and  $\eta = \eta_1$ , for  $\omega > m$ ; and  $t = [(m/\omega)^2 - 1]^{-1/2}$  and  $\eta = \eta_2$ , for  $\omega \leq m$ . So, when the acceleration  $a$  approaches zero,

$$\lim_{a \rightarrow 0} \Omega_a(m/\omega, a/\omega) = \begin{cases} \sqrt{1 - (m/\omega)^2}, & \omega > m, \\ 0, & \omega \leq m, \end{cases} \quad (\text{C9})$$

which is the results of a static quantum system in vacuum [41], as expected.

#### 4. The high-acceleration limit

For the high-acceleration limit where  $a \gg \omega$  and  $a \gg m$ , keeping only the lowest-order correction term, one finds that

$$\Omega_a(m/\omega, a/\omega) \approx 1 - \frac{m^2}{a^2} \left[ \left( \ln \frac{m}{a} \right)^2 - 1.23 \ln \frac{m}{a} + 0.63 \right], \quad (\text{C10})$$

which gives

$$\lim_{a \rightarrow \infty} \Omega_a(m/\omega, a/\omega) = 1. \quad (\text{C11})$$

#### Appendix D: The proof of $dC(\tau)/d\tau \leq 0$ when $\lambda = 0$

With the help of the evolution equations of density matrix elements (22), when  $\lambda = 0$ , the first derivative of  $K_{1(2)}(\tau)$  versus time  $\tau$  can be written as

$$\begin{aligned}\frac{dK_1(\tau)}{d\tau} &= [-\eta K_1(\tau) - f_1(\tau, \eta)] \Omega \Gamma_0, \\ \frac{dK_2(\tau)}{d\tau} &= [-\eta K_2(\tau) - f_2(\tau, \eta)] \Omega \Gamma_0,\end{aligned} \quad (\text{D1})$$

where the functions  $f_i(\tau, \eta)$  can be expressed as

$$\begin{aligned}f_1(\tau, \eta) &= \frac{[(\eta + 1) \rho_{EE}(\tau) + (\eta - 1) \rho_{GG}(\tau)][\rho_{AA}(\tau) + \rho_{SS}(\tau)]}{2\sqrt{\rho_{EE}(\tau)\rho_{GG}(\tau)}}, \\ f_2(\tau, \eta) &= \frac{[(\eta + 1) \rho_{EE}(\tau) + (\eta - 1) \rho_{GG}(\tau)][\rho_{AA}(\tau) + \rho_{SS}(\tau)]}{\sqrt{[\rho_{AA}(\tau) + \rho_{SS}(\tau)]^2 - [\rho_{AS}(\tau) + \rho_{SA}(\tau)]^2}}.\end{aligned} \quad (\text{D2})$$

It is obvious that  $f_1(\tau, \eta)$ ,  $f_2(\tau, \eta)$  are greater than or equal to 0. Therefore, it can be found from Eq. (D1) that, when  $\lambda = 0$ , if the concurrence  $C(\tau) > 0$ , i.e.,  $K_1(\tau) > 0$  or  $K_2(\tau) > 0$  ( $K_1(\tau)$  and  $K_2(\tau)$  cannot be greater than zero at the same time according to the definition of concurrence [48]), then  $dC(\tau)/d\tau \leq 0$ ; if the concurrence  $C(\tau) = 0$ , i.e.,  $K_1(\tau) \leq 0$  and  $K_2(\tau) \leq 0$ , then  $dC(\tau)/d\tau = 0$ .

### Appendix E: The limit properties of $\lambda_a(m/\omega, a/\omega, \omega L)$

The factor  $\lambda_a$  in Eq. (17) can be expressed in the following form

$$\begin{aligned} \lambda(m, a, L, \omega) &= \frac{\int_0^\infty \frac{k}{\sqrt{k^2+m^2/a^2}} K_{i2\omega/a} \left( 2\sqrt{k^2+m^2/a^2} \right) \frac{\sin(aLk)}{aL} dk}{\int_0^\infty \frac{k^2}{\sqrt{k^2+m^2/a^2}} K_{i2\omega/a} \left( 2\sqrt{k^2+m^2/a^2} \right) dk} \\ &= \frac{\int_0^\infty k K_{i\omega/a}^2 \left( \sqrt{k^2+m^2/a^2} \right) J_0(aLk) dk}{\int_0^\infty k K_{i\omega/a}^2 \left( \sqrt{k^2+m^2/a^2} \right) dk} \\ &= \frac{4a^2}{m^2} \frac{\int_{\frac{m}{a}}^\infty \frac{1}{aL} \sin(aL\sqrt{x^2-m^2/a^2}) K_{i2\omega/a}(2x) dx}{K_{1+i\omega/a}(m/a) K_{-1+i\omega/a}(m/a) - K_{i\omega/a}^2(m/a)}, \end{aligned} \quad (E1)$$

where  $J_\nu(x)$  and  $K_\nu(x)$  are the Bessel function of the first type and the modified Bessel function of the second type, respectively. The factor  $\lambda_a$  can be written as a function of dimensionless variables as  $\lambda_a(m/\omega, a/\omega, \omega L)$ .

#### 1. The low-mass limit

Keeping only the lowest-order term, in the low-mass limit where  $m \ll \omega$  and  $m \ll a$ , the limit of  $\lambda_a$  when  $m \rightarrow 0$  is

$$\lim_{m \rightarrow 0} \lambda_a(m/\omega, a/\omega, \omega L) = \frac{\sin\left(\frac{2\omega}{a} \sinh^{-1} \frac{aL}{2}\right)}{\omega L \sqrt{1 + a^2 L^2/4}},$$

which reduces to the result in the massless case.

#### 2. The high-mass limit

When  $m \gg a$  and  $m \gg \omega$ ,  $\lambda_a$  can be approximated as

$$\lambda_a(m/\omega, a/\omega, \omega L) \approx \frac{e^{-(\sqrt{4+a^2L^2}-2)\frac{m}{a}}}{1 + a^2 L^2/4}. \quad (E2)$$

Therefore, in the limit of  $m \rightarrow \infty$ ,  $\lambda_a$  is dependent on the value of  $aL$ .

$$\lim_{m \rightarrow \infty} \lambda_a(m/\omega, a/\omega, \omega L) = \begin{cases} 1, & aL = 0, \\ 0, & aL \neq 0. \end{cases} \quad (\text{E3})$$

### 3. The low-acceleration limit

If  $a \ll m$ ,  $a \ll \omega$  and  $a \ll 1/L$ ,

$$\lim_{a \rightarrow 0} \lambda_a(m/\omega, a/\omega, \omega L) = \begin{cases} \frac{\sin(L\sqrt{\omega^2 - m^2})}{L\sqrt{\omega^2 - m^2}}, & m/\omega < 1, \\ 1, & m/\omega \geq 1, \end{cases} \quad (\text{E4})$$

which reduces to the result in the vacuum case Eq. (20).

### 4. The high-acceleration limit

When  $a \gg m$ ,  $\lambda_a$  can be approximated as

$$\lambda_a(m/\omega, a/\omega, \omega L) \approx \frac{\sin\left(\frac{2\omega}{a} \sinh^{-1} \frac{aL}{2}\right)}{\omega L \sqrt{1 + a^2 L^2 / 4}}, \quad (\text{E5})$$

which is the result in the massless case. Based on this, if  $a \gg \omega$ , it can further be approximate as,

$$\lambda_a(m/\omega, a/\omega, \omega L) \approx \frac{4 \sinh^{-1} \left( \frac{aL}{2} \right)}{aL \sqrt{a^2 L^2 + 4}}. \quad (\text{E6})$$

Furthermore, if  $a \gg 1/L$ , then

$$\lambda_a(m/\omega, a/\omega, \omega L) \approx \frac{4 \log(aL)}{a^2 L^2}. \quad (\text{E7})$$

Here, if  $aL \ll 1$ , the approximate expression of  $\lambda_a$  can be written as  $\lambda_a \approx 1 - a^2 L^2 / 6$ . Thus, we can get the limit of  $\lambda_a$  when  $a \rightarrow \infty$  as

$$\lim_{a \rightarrow \infty} \lambda_a(m/\omega, a/\omega, \omega L) = \begin{cases} 1, & L = 0, \\ 0, & L \neq 0. \end{cases} \quad (\text{E8})$$

---

[1] S. A. Fulling, *Phys. Rev. D* **7**, 2850 (1973).

- [2] P. C. W. Davies, *J. Phys. A* **8**, 609 (1975).
- [3] W. G. Unruh, *Phys. Rev. D* **14**, 870 (1976).
- [4] L. C. B. Crispino, A. Higuchi, and G. E. A. Matsas, *Rev. Mod. Phys.* **80**, 787 (2008).
- [5] B. DeWitt, in *General Relativity: An Einstein Centenary Survey*, edited by S. W. Hawking and W. Israel (Cambridge University Press, Cambridge, England, 1980), p. 680.
- [6] S. Takagi, *Prog. Theor. Phys. Suppl.* **88**, 1 (1986).
- [7] J. Audretsch and R. Müller, *Phys. Rev. A* **50**, 1755 (1994).
- [8] H. Yu and S. Lu, *Phys. Rev. D* **72**, 064022 (2005).
- [9] Z. Zhu, H. Yu, and S. Lu, *Phys. Rev. D* **73**, 107501 (2006).
- [10] J. Audretsch and R. Müller, *Phys. Rev. A* **52**, 629 (1995).
- [11] R. Passante, *Phys. Rev. A* **57**, 1590 (1998).
- [12] L. Rizzato, M. Lattuca, J. Marino, A. Noto, S. Spagnolo, W. Zhou, and R. Passante, *Phys. Rev. A* **94**, 012121 (2016).
- [13] W. Zhou, R. Passante, L. Rizzato, *Phys. Rev. D* **94**, 105025 (2016).
- [14] L. Rizzato, *Phys. Rev. A* **76**, 062114 (2007).
- [15] Z. Zhu and H. Yu, *Phys. Rev. A* **82**, 042108 (2010).
- [16] J. Marino, A. Noto and R. Passante, *Phys. Rev. Lett.* **113**, 020403 (2014).
- [17] T. Yu and J. H. Eberly, *Phys. Rev. Lett.* **93**, 140404 (2004).
- [18] T. Yu and J. H. Eberly, *Science* **323**, 598 (2009).
- [19] Z. Ficek and R. Tanaś, *Phys. Rev. A* **74**, 024304 (2006).
- [20] D. Braun, *Phys. Rev. Lett.* **89**, 277901 (2002).
- [21] M. S. Kim, J. Lee, D. Ahn, and P. L. Knight, *Phys. Rev. A* **65**, 040101(R) (2002).
- [22] S. Schneider and G. J. Milburn, *Phys. Rev. A* **65**, 042107 (2002).
- [23] A. M. Basharov, *J. Exp. Theor. Phys.* **94**, 1070 (2002).
- [24] L. Jakóbczyk, *J. Phys. A* **35**, 6383 (2002).
- [25] B. Reznik, *Found. Phys.* **33**, 167 (2003).
- [26] F. Benatti, R. Floreanini, and M. Piani, *Phys. Rev. Lett.* **91**, 070402 (2003).
- [27] Z. Ficek and R. Tanaś, *J. Mod. Op.* **50**, 2765 (2003).
- [28] R. Tanaś and Z. Ficek, *J. Opt. B* **6**, S90 (2004).
- [29] R. Tanaś and Z. Ficek, *Phys. Scr.* **T140**, 014037 (2010).
- [30] Z. Ficek and R. Tanaś, *Phys. Rev. A* **77**, 054301 (2008).

- [31] L. Mazzola, S. Maniscalco, J. Piilo, K.-A. Suominen, and B. M. Garraway, *Phys. Rev. A* **79**, 042302 (2009).
- [32] S. Das and G. S. Agarwal, *J. Phys. B* **42**, 141003 (2009).
- [33] F. Benatti and R. Floreanini, *Phys. Rev. A* **70**, 012112 (2004).
- [34] J. Hu and H. Yu, *Phys. Rev. A* **91**, 012327 (2015).
- [35] Y. Yang, J. Hu, and H. Yu, *Phys. Rev. A* **94**, 032337 (2016).
- [36] S. Cheng, H. Yu, and J. Hu, *Phys. Rev. D* **98**, 025001 (2018).
- [37] J. Zhang and H. Yu, *Phys. Rev. D* **75**, 104014 (2007).
- [38] Y. Zhou, H. Yu, and Z. Zhu, *Commun. Theor. Phys.* **57**, 387 (2012).
- [39] W. Brenna, R. B. Mann and E. Martín-Martínez, *Phys. Lett. B* **757**, 307 (2016).
- [40] L. J. Garay, E. Martín-Martínez, and J. de Ramón, *Phys. Rev. D* **94**, 104048 (2016).
- [41] Y. Zhou, J. Hu, and H. Yu, [arXiv:2105.10646](https://arxiv.org/abs/2105.10646).
- [42] V. Gorini, A. Kossakowski and E. C. G. Sudarshan, *J. Math. Phys.* **17**, 821 (1976).
- [43] G. Lindblad, *Commun. Math. Phys.* **48**, 119 (1976).
- [44] R. Kubo, *J. Phys. Soc. Jpn.* **12**, 570 (1957).
- [45] P. C. Martin and J. Schwinger, *Phys. Rev.* **115**, 1342 (1959).
- [46] R. Haag, N. M. Hugenholtz and M. Winnink, *Commun. Math. Phys.* **5**, 215 (1967).
- [47] R. Tanaś, *Phys. Scr.* **T153**, 014059 (2013).
- [48] W. K. Wootters, *Phys. Rev. Lett.* **80**, 2245 (1998).
- [49] T. Li, B. Zhang, and L. You, *Phys. Rev. D* **97** 045005 (2018).